Momentum-resolved evolution of the Kondo lattice into 'hidden-order' in URu_2Si_2

F. L. Boariu,[1,*] C. Bareille,[2,*] H. Schwab,[1] A. Nuber,[1] P. Lejay,[3]
T. Durakiewicz,[4] F. Reinert,[1,5] and A. F. Santander-Syro[2,†]

[1] *Lehrstuhl für Experimentelle Physik VII, Universität Würzburg, Am Hubland, D-97074 Würzburg, Germany*
[2] *CSNSM, Université Paris-Sud and CNRS/IN2P3, Bâtiments 104 et 108, 91405 Orsay cedex, France*
[3] *Institut Néel, CNRS/UJF, B.P. 166, 38042 Grenoble Cedex 9, France*
[4] *MPA-CMMS, Los Alamos National Laboratory, Los Alamos, NM, USA*
[5] *Forschungszentrum Karlsruhe, Gemeinschaftslabor für Nanoanalythik, D-76021 Karlsruhe, Germany*

We study, using high-resolution angle-resolved photoemission spectroscopy, the evolution of the electronic structure in URu_2Si_2 at the Γ, Z and X high-symmetry points from the high-temperature Kondo-screened regime to the low-temperature 'hidden-order' (HO) state. At all temperatures and symmetry points, we find structures resulting from the hybridization between heavy and light bands, related to the Kondo lattice formation. Strikingly, we find that while the HO induces pronounced changes at Γ and Z, the electronic structure at X does not change. This explicitly demonstrates that the hidden-order parameter is anisotropic. Furthermore, our data show that the interaction of a light electron band with the Kondo-lattice characterizing the paramagnetic state leads to additional, momentum-dependent gaping in the ordered state. In particular, in the HO state, we observe the opening of a gap in momentum at the Γ and Z points.

The heavy-fermion URu_2Si_2 presents a second-order phase transition at $T_{HO} = 17.5$ K to a 'hidden order' (HO) state of yet unknown order parameter [1–3]. The 27-year quest for an understanding of this transition has triggered an extensive research [4–35] (for a recent review, see Ref. [36]). The electronic properties of this material are determined by the dual 'itinerant-localized' character of the uranium $5f$ electrons, with Kondo screening developing below $T \sim 70$ K, as inferred from transport data [1, 2]. Earlier angle-resolved photoemission spectroscopy (ARPES) experiments indicated the presence, in the paramagnetic (PM) state, of an f-like feature at the Fermi level near the X point [37, 38], while optical conductivity data showed that a Drude peak forms below 75 K and narrows as temperature decreases, consistent with metallic behaviour [39–42]. Thus, a crucial aspect of the HO is that it emerges on a pre-formed Kondo lattice. Indeed, recent high-resolution ARPES and STM experiments demonstrated that itinerant heavy quasi-particles participate in the Fermi-surface instability that leads the HO state [21, 24–26]. However, to date, there is no momentum-resolved picture spanning several high-symmetry points showing how the electronic structure evolves from the Kondo-screened to the HO state.

In this work, we demonstrate the existence of distinct heavy-fermion features at the Γ, Z and X points of URu_2Si_2 up to temperatures close to the onset of Kondo screening. We show that these structures result from the hybridization between heavy and light bands, and can be thus linked to the formation of the Kondo-lattice. We find that the HO transition shifts the Kondo-lattice structures at the Γ and Z points well below the Fermi level, while leaving unchanged the electronic structure at X, explicitly showing that the order parameter does not affect equally all the bands near E_F. Additionally, we observe that in the HO state, the heavy-fermion bands at Γ and Z become gapped in momentum at E_F. We provide a phenomenological model to describe the electronic structure at Γ, Z and X and its evolution from the Kondo lattice to the HO state. In particular, we show that a light electron band (LEB), interacting with the Kondo-lattice heavy-fermions, is an essential ingredient to understand the observations below T_{HO} at Γ and Z.

The high-resolution ARPES experiments were performed with Scienta R4000 detectors at Würzburg University, using monochromatized He-I$_\alpha$ ($h\nu = 21.2$ eV, resolution 5.18 meV) and Xe-I ($h\nu = 8.4$ eV, resolution ~ 4 meV) photons from an MBS T-1 multi-gas discharge lamp, and at the UE112-PGM-1b ("1^3") beamline of the Helmholtz Zentrum Berlin (HZB) – BESSY-II using

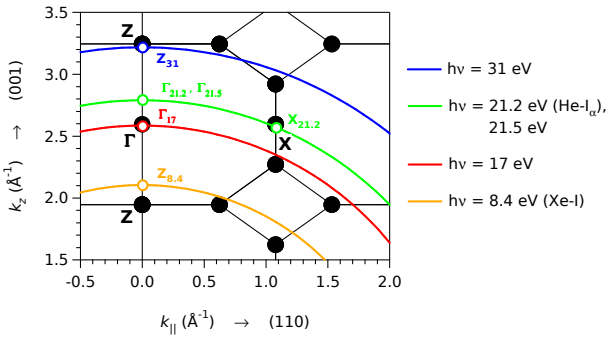

FIG. 1. (Color online) Body-centered tetragonal Brillouin zone (black lines) and ARPES measurement arcs in momentum space (color lines) for photon energies of 8.4 eV (Xe-I), 17 eV, 21.2 eV (He-Iα), 21.5 eV and 31 eV. Open circles show the measurement points discussed in the main text. The index of each measurement point refers to the photon energy in eV. The arcs were obtained from a model of a free-electron final state with an inner potential $V_0 = 13$ eV [37].

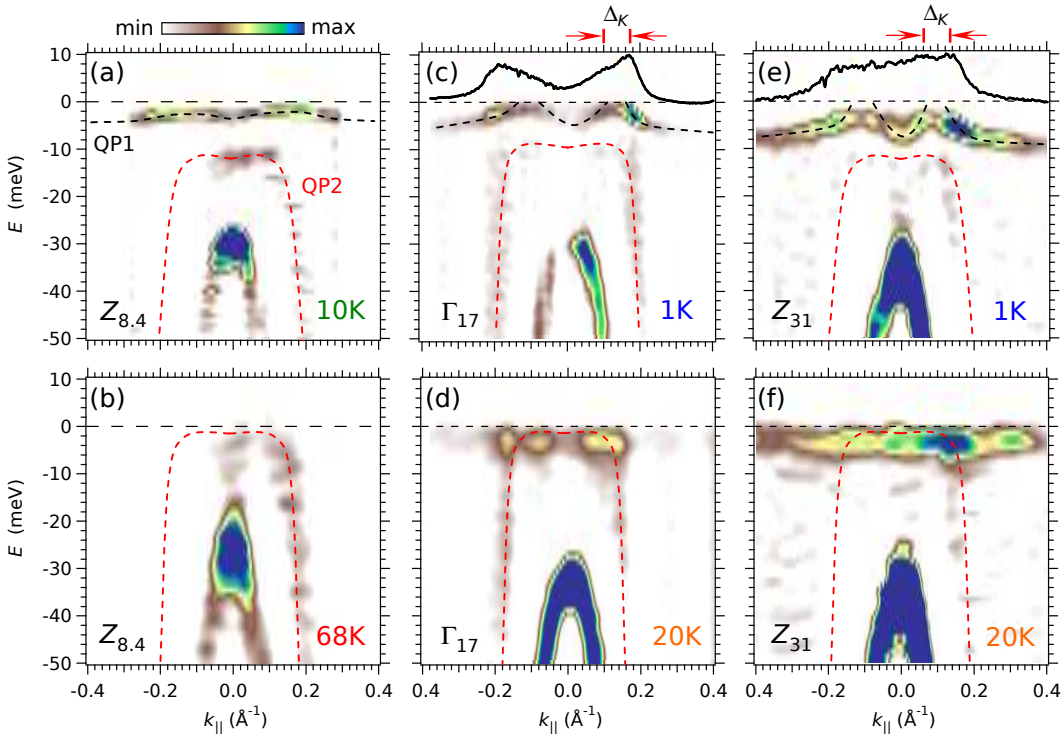

FIG. 2. (Color online) (a, b) Second derivative of ARPES data at the $Z_{8.4}$ point, at 10 K and 68 K respectively. (c, d) Second derivative of ARPES data at Γ_{17}, at 1 K and 20 K respectively. (e, f) Corresponding data at the Z_{31} point. In panels (c) and (e), the black solid curves show the MDCs integrated over 5 meV around E_F. A gap in momentum $\Delta_k \approx 0.08 \pm 0.01$ Å^{-1} is indicated by the red arrows. In all panels, the black and red dashed lines are guides to the eye for QP1 and QP2, respectively, and the measurement direction is (110).

horizontally-polarized light at $h\nu$ = 17, 21.5 and 31 eV (resolution 3 meV). Measurements at different photon energies correspond to different values of k_z along (001) [43]. In what follows, the measurement points will be labeled as in Fig. 1. The samples were cleaved *in-situ* along the (001) axis at 10 K (Würzburg) and 1 K (BESSY), and measured along the (110) (or $k_{||}$) direction. The pressure was below 5×10^{-11} Torr at BESSY and when using the Xe-lamp, separated from the measurement chamber by a MgF_2 window, and of 5×10^{-10} Torr when using the He-lamp. We checked that, apart from thermal broadening, the spectra at 1 K and 5 K are identical, so that any changes that might be induced by the superconducting transition at 1.2 K do not affect our discussions below.

We discuss first the evolution of the electronic structure near E_F across the HO transition at different high-symmetry points. Figures 2(a, b) show the electronic structure at $Z_{8.4}$ as second derivatives of the ARPES data in the HO (10 K) and PM (68 K) states (the raw data and details of the second derivative calculations are presented in the Supplemental Material). The intense surface state below −30 meV and a light hole band (LHB) parallel to it were described previously [21, 24, 44, 45]. Furthermore, the data at 10 K in Fig. 2(a) show a heavy quasi-particle band dispersing down to $E = -3$ meV at $k_{||} = 0$ (hereafter QP1, black dashed lines), and a second, essentially flat band at $E = -10$ meV (QP2, red dashed lines) between ± 0.15 Å^{-1}, in agreement with laser-ARPES studies of the Z-point in URu_2Si_2 [24, 45, 46]. QP1 has an "M-shaped" dispersion, discussed later. A crucial novel aspect of our data is the clearly visible onset of dispersion of QP2 due to hybridization with the above LHB: following the flat region around $k_{||} = 0$, at momenta larger than ~ 0.15 Å^{-1}, QP2 merges with LHB, forming a whole single "Π-shaped" structure that is gapped with respect the Fermi level (E_F). The existence and formation of such a coherence hybridization gap has been recently studied in the case of $4f$ and $5f$ systems [47–49]. Thus, our work provides a direct imaging of the hybridization gap in URu_2Si_2, which was so far observed only indirectly with optical methods [39, 50]. As we will show further, similar structures are observed in the Γ and X points. Also new in our data is that, as shown in Fig. 2(b), the "Π-shaped" structure exists at temperatures as high as 68 K, close to the onset of Kondo screening, while previous ARPES studies at the Z-point claimed that above T_{HO} all features dissapeared or were not detectable [24, 45, 46]. However, in contrast to the HO state, at 68 K the binding energy of QP2 is now $\approx E_F$, and QP1 is not detected anymore –either because it shifted above E_F or because it merged with QP2. Previous reports have shown that, in the HO state, both QP1

and QP2 shift towards E_F as temperatures rises towards T_{HO} [46]. The data of figures 2(a b), plus data discussed next confirm this picture, and demonstrate that at all temperatures above T_{HO} and up to 68 K, one observes only the peak of QP2 around E_F, its binding energy remaining essentially temperature-independent.

Figures 2(c, d) show the second-derivative spectra at the Γ_{17} point at 1 K and 20 K, respectively. The corresponding data at Z_{31} is presented in figures 2(e, f). Figs. 2(a, c, e) show that, in the HO state, QP1 and QP2 exist both at the Z and Γ points. This demonstrates that QP2 is *not* an exclusive feature of the Z point [46], but rather a general feature of the elecronic structure along $\Gamma - Z$. Later on, we will show that QP1 and QP2 can be understood on the common framework of the evolution of the Kondo lattice across the HO transition. At the lowest measured temperature of 1 K, the energies of QP1 and QP2 at $k_{\|} = 0$ are $E_{\rm QP1} = -5.5 \pm 0.5$ meV and $E_{\rm QP2} = -12 \pm 1$ meV, respectively. Note that the temperature-induced energy shifts of both QP1 and QP2, observed from panels at different temperatures in Fig. 2, and also reported elsewhere [46], indicate that both structures are related to the bulk physics of the HO transition. More important, the ultra-low temperature and high-resolution measurements of Figs. 2(c, e) (see also the Supplemental Material) distinctly show that, at E_F, the M-shaped dispersion of QP1 becomes *gapped in momentum* both at Γ and Z, cutting through the Fermi level at two different Fermi momenta, such that the tips of the "M" lie above E_F: $k_F^{inner} \approx \pm 0.06$ Å^{-1} and $k_F^{outer} \approx \pm 0.14$ Å^{-1}. On the other hand, at $T > T_{HO}$, Figs. 2(b, d, f) show that the "Π-shaped" structure ascribed to QP2 has shifted at or near E_F for the three values of k_z. In particular, at Z_{31} in Fig. 2(f) (see also the raw data in the Supplemental Material), one still distinguishes traces of the high-momenta wings of QP1's M-like dispersion, due to the thermal broadening of these states lying now at or slightly above E_F, not well below E_F as in the HO phase [Fig. 2(e)]. Consequently, the momentum gap observed in the HO phase closes.

Figures 3(a, b) present the ARPES data at the $X_{21.2}$ point in the PM (22 K) and HO (10 K) states, respectively. Division by a Fermi-Dirac distribution of appropriate effective temperature [21] shows that, at both temperatures, the electronic structure corresponds to the hybridization of a LHB and a heavy electron band (HEB, dashed white lines, see later). In particular, the data distinctly show the dispersing wings of the HEB occurring *right above* E_F. Additionally, figure 3 (c) shows that the experimental energy gap between the maximum of the lower hybridized band and the minimum of the upper hybridized band is essentially temperature-independent and of the order of 10 meV. Thus, contrary to Γ and Z, at X the electronic structure is *not* affected by the HO transition. This is consistent with the HO gap being *anisotropic* along the Fermi surface, as suggested by

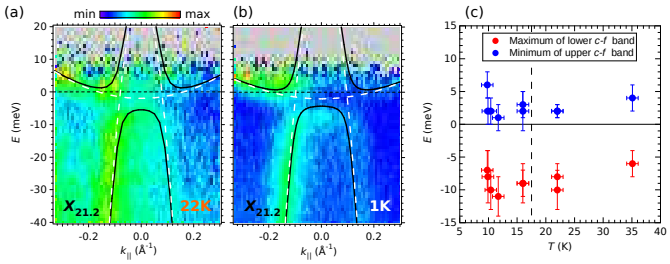

FIG. 3. (Color online) (a, b) Energy-momentum ARPES intensity maps at the X point of URu_2Si_2, using He-I$_\alpha$ photons in the PM (22 K) and and HO (10 K) phases, respectively. The data have been normalized to the Fermi-Dirac distribution of a metallic reference at the same temperature and in electrical contact with the sample, measured under identical conditions [21]. Intensity differences between left and right image halves are attributed to matrix elements changing at X when going across neighboring Brillouin zones. Overlaid on the ARPES maps are the original (dashed white lines) and hybridized (solid black lines) bands used to fit the data (see main text). (c) Experimental values of the energy-maximum of the lower hybridized structure (red circles) and the energy-minimum of the upper hybridized structure (blue circles) as a function of temperature across the HO transition.

thermo-transport [2, 17], tunneling [11] and optical measurements [39, 42].

We now introduce a phenomenological model to describe the evolution of the electronic structure at Γ, Z and X from the Kondo lattice regime into the HO state. We start with the data at X, simpler than at Γ or Z. It can be fitted by a standard hybridization model (see *e.g.* Ref. [51]) between a LHB of mass $\sim -0.9 m_e$ (m_e is the free-electron mass) and a HEB of mass $\sim 50 - 70 m_e$ interacting through a potential $V_{he}^X \approx 11$ meV. The resulting "upper" and "lower" hybridized bands are shown by the solid black lines in Figures 3(a, b).

Based on the above two-band hybridization at X, we now suggest a toy model for the spectra near Γ and Z to capture the ingredients essential to describe the observed changes across the HO transition. For definiteness, we concentrate on the data at Z_{31}. Figure 4(a) shows the second derivative of the ARPES data at Z_{31} in the PM (20 K) phase after being normalized by the Fermi-Dirac distribution (corresponding raw data in the Supplemental Material). This puts in evidence the wings of a HEB dispersing close to E_F, confirming the observations described in Fig. 2(f), and supporting a scenario for the PM state based on the hybridization of a HEB and the previously described LHB. Furthermore, from the data at 1 K in Fig. 2(e), reproduced for clarity in the discussion in figure 4(b), we note that in the HO state two additional ingredients are needed to reproduce the M-shaped dispersion of QP1: a strong renormalization (down-shift in energy) of the HEB, to account for the high-momenta wings of QP1 now lying well below E_F, and the introduction of a LEB, to account for its dispersion near $k_{\|} = 0$.

We assume that the hybridization potential between

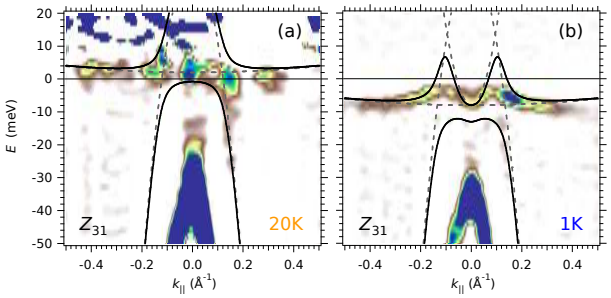

FIG. 4. (Color online) (a, b) ARPES data at Z_{31} in the PM (20 K) and HO (1 K) phases, corresponding to the data in figures 2(e, f), compared to the phenomenological model for the "original" (dotted lines) and hybridized (solid lines) bands accounting for the dispersions of QP1 and QP2 in the HO phase (see main text). The upper part of the hybridized structure between the LEB and LHB lies out of the figure scale.

the HEB and the LHB is due to the onset of Kondo coherence at much higher temperature, and thus remains constant across the HO transition. The proposed non-hybridized bands are represented by the dashed lines in figures 4(a, b), and the resulting hybridized bands by the black solid lines. Thus, at $T > T_{HO}$ in Fig. 4(a), the bottom of the HEB sits at or a few meV above E_F. Its hybridization with the LHB gives the observed Π-shaped structure at E_F and another structure above E_F, of which we can only observe the heavy electron wings. Well below T_{HO}, in Fig. 4(b), the HEB has dropped below E_F, reaching its minimum at -8 meV. A LEB, now clearly present below E_F, interacts with the previoulsy hybridized LHB and HEB, and one distinctly observes the Π-shaped QP2 and the M-shaped QP1. At this temperature, the best fit is obtained with a LHB of mass $\approx -1.6m_e$ and top energy of about 35 meV hybridizing with a doublet, essentially degenerate at Z, composed of the HEB (mass $\gtrsim 500m_e$) and the LEB of mass similar to LHB, through a hybridization potential $V \approx 11$ meV.

The main, robust insight from the model above is that to understand the dispersion of QP1 close to $k_{||} = 0$ below T_{HO}, it is essential to consider a LEB interacting with the LHB and HEB observed above T_{HO}. This also explains why QP1 and QP2 shift by the same amount below T_{HO} [46]: the hybridization interaction with the LEB repels QP2. The model does not reproduce the positive curvature of the QP1 wings at high momenta, possibly indicating that a more realistic tight-binding dispersion should be used for the HEB. Similarly, the energy at Z of the HEB and LEB in the PM state cannot be accurately determined, because details of the bands above E_F cannot be inferred from our data.

Conservation of particles requires that, in the PM state, the LEB be already present below E_F, possibly at a different region in momentum. Where this band comes from, and why the HEB drops, are open questions. One possibility is band nesting or folding [19, 22, 31, 34, 35]. We note however that, in standard nesting or folding, one band is folded "rigidly" onto another [52]: its binding energy does not shift gradually with temperature, contrary to the observations, and only the gap between the original and folded bands changes.

Our results demonstrate that the HO transition is intimately related to the Kondo lattice of heavy-fermions in URu_2Si_2, that we observe up to temperatures close to the onset of coherence. Furthermore, our data explicitly show that the Fermi-surface instability induced by the HO on the Kondo lattice [21] affects differently the electronic structure at various high-symmetry points, opening a gap in momentum at Γ and Z. Regardless of the mechanism behind the HO transition, this gap in momentum implies the existence of a gap in energy between the two bands being separated, that should occur at E_F at other places in reciprocal space. Our model above indicates that such a gap is of the order of 10 meV, in agreement with transport experiments [2, 39]. Crucially, our data analysis strongly suggests that the HO transition is related to the interaction between the lattice of heavy-fermions and a band of light electrons, thus opening gaps in the electronic structure near E_F. All these observations put strong constrains on theories for the HO transition.

We thank C. Pépin, M.-A. Méasson and S. Burdin for fruitful discussions, the HZB for the allocation of synchrotron radiation beamtime, and E. Rienks and T. Setti for their invaluable help during beamtime. The work at Würzburg is supported by the Deutsche Forschungsgemeinschaft through FOR1162. TD was supported by the U.S. DOE. AFSS acknowledges support from the Institut Universitaire de France.

SUPPLEMENTAL MATERIAL

Raw data at $Z_{8.4}$

Figures 5(a, b) present the raw data for the electronic structure at $Z_{8.4}$, *i.e.*, using Xe-I photons, as momentum-resolved stacks of energy distribution curves (EDCs) in the HO (10 K) and PM (68 K) states. The surface state below -30 meV [21, 44], and the "M-shaped" QP1 and "Π-shaped" QP2", described in the main text, are all observed in these figures. Note in particular, in panel (a), the clear onset of dispersion of QP2 at momenta larger than ~ 0.15 Å^{-1}, corresponding to hybridization of a heavy electron band with a light hole band, as described in the main text. Note also, from panel (b), how the flat, non-dispersive part of QP2 has effectively shifted to $\approx E_F$ at 68 K.

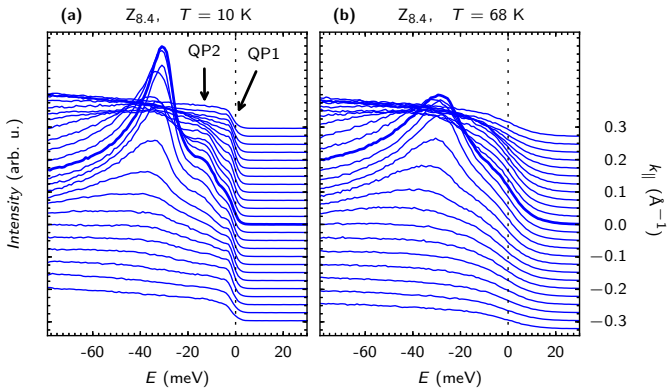

FIG. 5. (a, b) EDC stacks of ARPES data at $Z_{8.4}$, using Xe-I photons, at 10 K and 68 K respectively. The measurement direction is (110). QP1 and QP2 (main text) are shown by the markers and arrows in panel (a). The values of $k_{\parallel}$ shown at the right-hand side scale refer to the baseline (zero-intensity level well above E_F) of the spectra. The bold EDCs correspond to $k_{\parallel} = 0$

Raw data at the Γ_{17}, $\Gamma_{21.5}$ and Z_{31} points

Figure 6 shows the raw energy-momentum ARPES intensity maps at 1 K (top row panels) and 20 K (bottom row) for three different photon energies corresponding to the Γ_{17} (left column), $\Gamma_{21.5}$ (middle column) and Z_{31} (right column) points.

The fine features of the spectra are best observed by representing the data as EDC stacks, as shown in figure 7. At 1 K, Figs. 7(a-c), both QP1 and QP2 are observed at the three values of k_z. Additionally, near $k_{\parallel} = 0$, the EDCs of QP1 show evidence for a splitting into a fine double-peak structure, best observed at the $\Gamma_{21.5}$ and Z_{31} points in Figs. 7(b, c). A similar fine splitting was recently observed by laser-ARPES at the $Z_{7.0}$ point [46]. Thus, our data shows that such fine splitting also exists at the Γ point.

Note, from figures 6(a-c) and 7(a-c), that QP1 clearly disperses through E_F, yielding a gap in momentum $\Delta_k \approx 0.08 \pm 0.01$ Å^{-1}, described in the main text.

At $T > T_{HO}$, Figs. 7(d-f), the "Π-shaped" structure ascribed to QP2 shifts to $E \approx E_F$ for the three values of k_z. Moreover, the 20 K data at Γ_{17} and Z_{31} also show that the upper part of QP2's Π-shaped structure has actually an electron-like character, in agreement with the hybridization model presented in the main text. Additionally, as can be seen in Fig. 7(f), at 20 K the high-momenta wings of QP1's M-like dispersion still give a finite spectral weight at E_F, indicating that the heavy band forming QP1, which was located well below E_F in the HO phase [Fig. 7(c)], has now shifted to energies slightly above E_F, thus closing the momentum gap observed in the HO phase.

Raw data at Z_{31} and band-hybridization model

Figures 8(a, b) show, over a larger energy range, the raw ARPES intensity maps at Z_{31} in the PM (20 K) and HO (1 K) phases. The data at 20 K, normalized by the Fermi-Dirac distribution, shows the wings of a HEB dispersing close to E_F. As discussed in the main text, this supports our hybridization model. The proposed non-hybridized bands are represented by the dashed lines in figures 8(a, b), and the resulting hybridized bands by the black solid lines.

Procedure of second-derivative rendering

The raw photoemission intensity maps were convoluted with a two-dimensional Gaussian of widths $\sigma_E = 3$ meV and $\sigma_k = 0.06$ Å^{-1} for temperatures below 10 K, and $\sigma_E = 5$ meV and $\sigma_k = 0.08$ Å^{-1} for $T > 10$ K. Second derivatives along the E_B and $k_{\parallel}$ axes were normalized to the maximum intensity of the surface state peak, then averaged. Only negative intensity values, which represent peak maxima in the original data, are shown in the main text.

* F.L.B. and C.B. contributed equally to this work
† andres.santander@csnsm.in2p3.fr

[1] T. T. M. Palstra *et al.*, Phys. Rev. Lett. **55**, 2727-2730 (1985).
[2] M. B. Maple *et al.*, Phys. Rev. Lett. **56**, 185-188 (1986).
[3] W. Schlabitz *et al.*, Zeitschrift fur Physik B **62**, 171-177 (1986).
[4] C. Broholm *et al.*, Phys. Rev. Lett. **58**, 1467-1470 (1987).
[5] J. Schoenes *et al.*, Phys. Rev. B **35**, 5375-5378 (1987).
[6] A. Ler Dawson, W. S. Datars, J. D. Garrett, and F. S. Razavi. J. Phys. Condens. Matter **1**, 6817-6828(1989).
[7] T. E. Mason and W. J. L. Buyers. Phys. Rev. B **43**, 11471-11473 (1991).
[8] C. Broholm *et al.*, Phys. Rev. B **43**, 12809-12822 (1991).
[9] P. Santini and G. Amoretti. Phys. Rev. Lett. **73**, 1027-1030 (1994).
[10] W. J. L. Buyers *et al.*, Physica B **199-200**, 95-97 (1994).
[11] R. Escudero, F. Morales, and P. Lejay, Phys. Rev. B **49**, 15271-15275 (1994).
[12] H. Amitsuka *et al.*, Phys. Rev. Lett. **83**, 5114-5117 (1999).
[13] P. Chandra, P. Coleman, and J. A. Mydosh. Physica B **312-313**, 397-400 (2002).
[14] P. Chandra, P. Coleman, J. A. Mydosh, and V. Tripathi. Nature **417**, 831-834 (2002).
[15] F. Bourdarot *et al.*, Phys. Rev. Lett. **90**,067203 (2003).
[16] C. R. Wiebe *et al.*, Phys. Rev. B **69**, 132418 (2004).
[17] K. Behnia *et al.*, Phys. Rev. Lett. **94**, 156405 (2005).
[18] C. R. Wiebe *et al.*, Nature Phys. **3**, 96-100 (2007).
[19] S. Elgazzar *et al.*, Nature Mater. **8**, 337-341 (2009).
[20] J. A. Janik *et al.*, J. Phys. Condens. Matter **21**, 192202 (2009).

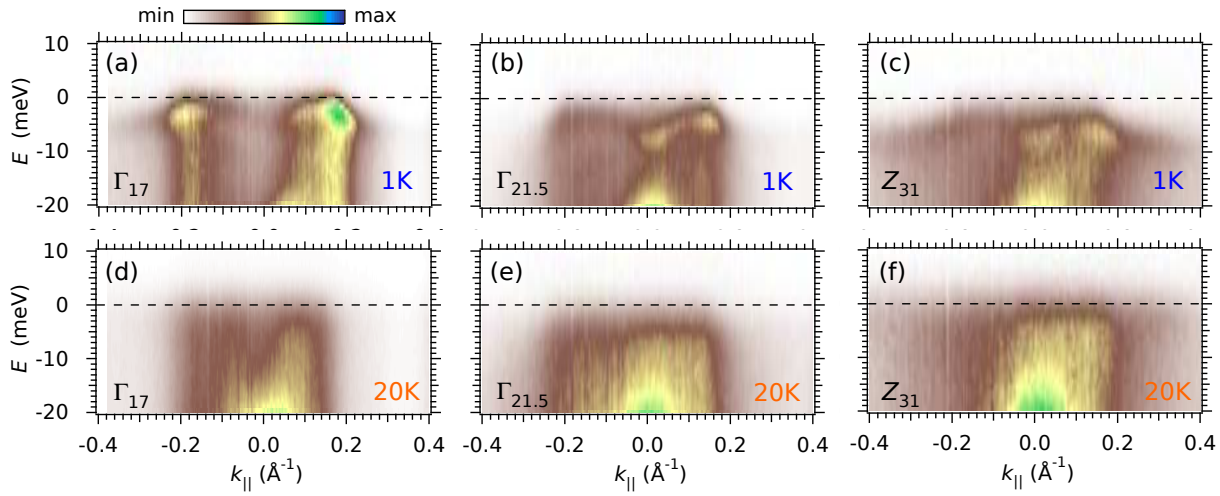

FIG. 6. (a-c) Energy-momentum ARPES intensity maps in the HO state (1 K) at the Γ_{17}, $\Gamma_{21.5}$ and Z_{31} points, respectively. (d-f) Corresponding data in the PM state (20 K).

[21] A.F. Santander-Syro *et al.*, Nature Phys. **5**, 637-641 (2009).
[22] K. Haule and G. Kotliar. Nature Phys. **5**, 796-799 (2009).
[23] K. Haule and G. Kotliar. EPL **89**, 57006 (2010).
[24] R. Yoshida *et al.*, Phys. Rev. B **82**, 205108 (2010).
[25] A. R. Schmidt *et al.*, Nature **465**, 570-576 (2010).
[26] P. Aynajian *et al.*, PNAS **107**, 10383-10388 (2010).
[27] P. M. Oppeneer *et al.*, Phys. Rev. B **82**, 205103 (2010).
[28] P. M. Oppeneer *et al.*, Phys. Rev. B **84**, 241102 (2011).
[29] I. Kawasaki *et al.*, Phys. Rev. B **83**, 235121 (2011).
[30] G. L. Dakovski *et al.*, Phys. Rev. B **84**, 161103 (2011).
[31] Y. Dubi and A. V. Balatsky, Phys. Rev. Lett. **106**, 086401 (2011).
[32] J. T. Haraldsen, Y. Dubi, N. J. Curro, and A. V. Balatsky, Phys. Rev. B **84**, 214410 (2011).
[33] C. Pépin, M. R. Norman, S. Burdin, and A. Ferraz, Phys. Rev. Lett. **106**, 106601 (2011).
[34] P. S. Riseborough, B. Coqblin, and S. G. Magalhães, Phys. Rev. B **85**, 165116 (2012).
[35] P. Chandra, P. Coleman, and R. Flint, arXiv:1207.4828 (2012).
[36] J. A. Mydosh and P. M. Oppeneer, Rev. Mod. Phys. **83**, 1301 (2011).
[37] J. D. Denlinger *et al.*, Physica B **281-282**, 716-722 (2000).
[38] J. D. Denlinger *et al.*, J. Electron Spectrosc. **117-118**, 347-369, 2001.
[39] D. A. Bonn *et al.*, Phys. Rev. Lett. **61**, 1305-1308 (1988).
[40] J. Levallois *et al.*, Phys. Rev. B **84**, 184420 (2011).
[41] U. Nagel *et al.*, arXiv:1107.5574v1 [cond-mat.str-el] (2011).
[42] J. S. Hall *et al.*, Phys. Rev. B **86**, 035132 (2012).
[43] S. Hüfner. Photoelectron spectroscopy: principles and applications. Third edition, Springer (2003).
[44] F. L. Boariu *et al.*, J. Electron Spectrosc. **181**, 82-87 (2010).
[45] R. Yoshida *et al.*, J. Phys. Chem. Solids **72**, 580-581 (2011).
[46] R. Yoshida *et al.*, Phys. Rev. B **85**, 241102 (2012).
[47] D.V. Vyalikh *et al.*, Phys. Rev. Lett. **103**, 137601 (2009).
[48] M. Klein *et al.*, Phys. Rev. Lett. **106**, 186407 (2011).
[49] X. Yang, P. S. Riseborough, and T. Durakiewicz, J. Phys.: Condens. Matter **23**, 094211 (2011).
[50] M. K. Liu *et al.*, Phys. Rev. B **84**, 161101(R) (2011).
[51] P. Misra. Heavy-fermion systems. Handbook of Metal Physics (Series Editor: P. Misra), Elsevier (2008).
[52] A. F. Santander-Syro *et al.*, Phys. Rev. Lett. **106**, 197002 (2011).

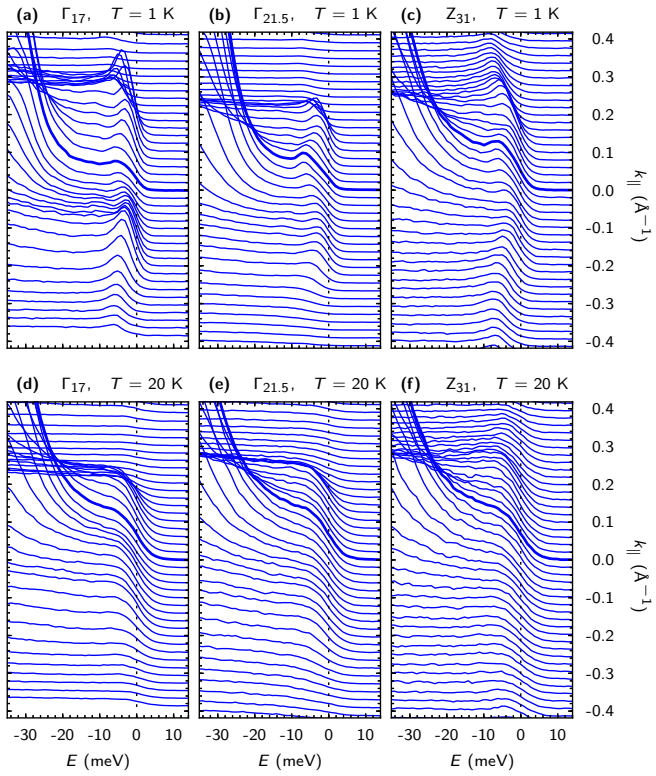

FIG. 7. (a-c) EDC stacks of ARPES data in the HO state (1 K) at the Γ_{17}, $\Gamma_{21.5}$ and Z_{31} points, respectively. (d-f) Corresponding stacks in the PM state (20 K). The values of $k_{\|}$, referred to the baseline of the spectra, are shown at the right-hand side scale. The bold EDCs denote $k_{\|} = 0$. All the EDCs in this figure were extracted from the intensity maps shown in figure 6.

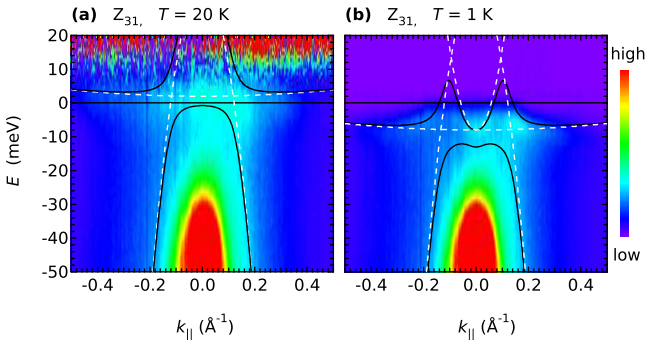

FIG. 8. (a, b) ARPES intensity maps at Z_{31} in the PM (20 K) and HO (1 K) phases, respectively, corresponding to the EDC stack from Figs. 7(c, f). Dotted and solid lines represent, accordingly, the "original" and hybridized bands of the scenario accounting for the dispersions of QP1 and QP2 in the HO phase (see main text). The upper part of the hybridized structure between the LEB and LHB lies out of the figure scale.